of arachidonate, displaying EC_{50} values of 1.9 and 15 μM, respectively, at 6 μM arachidonate concentration (35 °C).[9]

Kinetic studies with **9** showed that it inhibits the 5-LO enzyme (Table I) less well than **4** as expected from previous work.[7]

The 5-LO inhibitory action of **7** and **8** prompted the study of an entirely different metal-chelating analogue of arachidonate, the 2,3-dihydroxybenzamide derivative **10**. The 2,3-dihydroxybenzoyl group is known to possess high affinity for Fe(III). In fact, **10** was found to be a potent 5-LO inhibitor, with EC_{50} of 10 μM.[10]

Since a number of antioxidants that serve as hydrogen atom donors can function as lipoxygenase inhibitors,[11] the phenolic arachidonamide **11** was synthesized and tested as a 5-LO inhibitor. It proved to have activity (Table I), but it was considerably less effective than the hydroxamates **4-6**.

The studies reported herein provide important new guidance for the design of potent leukotriene biosynthesis inhibitors.[12,13]

(9) The synthesis of **7** was accomplished from 3(*Z*),6-heptadien-1-ol via the corresponding triphenylphosphonium bromide through a Wittig coupling with methyl 4-formylbutyrate (6:1 tetrahydrofuran–hexamethylphosphoric triamide at −78 °C) and subsequent conversion of the resultant methyl ester to **7** using hydroxylamine–sodium methoxide in methanol at 25 °C. The synthesis of **8** was conducted in a similar way starting with (2-phenylethyl)-triphenylphosphonium bromide and methyl 4-formylbutyrate.

(10) The synthesis of **10** was carried out from methyl 10-aminodeca-5-(*Z*),8(*Z*)-dienoate by (1) reaction with the cyclic sulfite of 2,3-dihydroxybenzoyl chloride (from the dihydroxybenzoic acid and thionyl chloride) and (2) hydrolysis with lithium hydroxide in tetrahydrofuran–water at 20 °C. The aminodecadienoate ester was synthesized from $THPOCH_2C{\equiv}CCH_2CH_2OH$ by the sequence (1) $CH_2OH \rightarrow CH_2I \rightarrow CH_2P^+Ph_3I^-$, (2) Wittig coupling of the phosphonium iodide with methyl 4-formylbutyrate, (3) CH_2–OTHP $\rightarrow CH_2OH \rightarrow CH_2OSO_2CH_3 \rightarrow CH_2N_3 \rightarrow CH_2NH_2$, and (4) hydrogenation of C≡C to *cis*-CH=CH using Lindlar catalyst.

(11) Lombardino, J. G. *Annu. Rep. Med. Chem.* **1981**, *16*, 189.

(12) For previous work on hydroxamic acids as inhibitors of zinc metalloproteases, see: Nashino, N.; Powers, J. C. *J. Biol. Chem.* **1980**, *255*, 3482 and references cited therein.

(13) This research was supported in part by the National Institutes of Health and the National Science Foundation.

Table I[a]

% RuO_2	$\chi_m(RuO_2) \times 10^6$	$\mu(RuO_2)$	T, K
10.0	223	0.52	150.8
	200	0.56	199.0
	185	0.60	247.1
	178	0.65	295.1
7.5	337	0.64	151.1
	296	0.69	199.3
	273	0.73	247.5
	260	0.78	295.4
5.0	488	0.77	150.6
	425	0.82	198.7
	385	0.87	246.9
	365	0.93	295.1
3.0	332	0.63	149.8
	286	0.67	198.2
	256	0.71	246.5
	244	0.76	294.6
2.0	378	0.67	150.6
	315	0.71	198.8
	276	0.74	247.0
	264	0.79	294.9
1.0	450	0.74	150.8
	372	0.77	198.9
	317	0.79	247.0
	378	0.94	295.0
pure RuO_2,	165		149.0
ref 9, p 341	164		163.0
	165		190.0
	164		236.0
	165		255.0
	168		297.0

[a] $\chi_g(TiO_2) = 0.043 \times 10^{-6}$ cgsu/g (Figure 1). $\chi_g^{dia}(RuO_2) = -0.323 \times 10^{-6}$ cgsu/g (ref 9).

Quantitative Studies on the Paramagnetic Behavior of RuO_2–TiO_2 (Anatase) Powders Catalytically Active in Water Oxidation

P. Baltzer,[†] R. S. Davidson,[‡] A. C. Tseung,[‡] M. Grätzel,[§] and J. Kiwi*

Anorganisch-Chemisches Institut Universität Zürich
8057 Zürich, Winterthurerst 190, Switzerland
Department of Chemistry, The City University
Northampton Square, London EC1V 4PB, England
Institut de Chimie-Physique
Ecole Polytechnique Fédérale
CH-1015 Lausanne, Switzerland
Received August 15, 1983

Transition-metal ion such as Ce^{4+} and Fe^{3+} in $HClO_4$ media oxidize water[1] to oxygen upon photolysis in a photoassisted reaction. Ce^{4+} in the presence of a macrodisperse RuO_2 redox catalyst[2-4] (in the dark) has been shown to be capable of oxidizing water as shown by eq 1. Recently, studies on RuO_2 systems

$$4Ce^{4+} + 2H_2O \xrightarrow{RuO_2\ catalyst} 4Ce^{3+} + 4H^+ + O_2 \qquad (1)$$

stabilized by TiO_2[5] have shown that TiO_2 is a suitable host to stabilize RuO_2. The purpose of this communication is to report in detail the paramagnetic properties of RuO_2–TiO_2 powders which are catalytically active in mediating water oxidation. The necessity of examining more closely the nature of these surfaces arises from the fact that the exact nature of the material intervening in the reaction determines the observed efficiency in water cleavage.[2,4,5]

Magnetic susceptibility of the samples was measured with a Faraday balance from Oxford Instruments. All powder samples were mechanically pressed to avoid alignment along a principal magnetization axis of the crystallites in the powder parallel to the applied magnetic field.[6] Thirty-milligram samples were sufficient to obtain sizeable effects, and all measurements were carried out in a field of 5.41 T with gradients of 0.3, 0.5, and 0.7 T/cm. The magnetic field was calibrated with $HgCo(NCS)_4$ at 273 K.[7] In the present study, chemical hydrolysis of $RuCl_3$ under controlled conditions has been used to produce islands of ruthenium dioxide. Details of this preparation have been previously reported.[5e]

Figure 1 shows the magnetic susceptibility (χ_g') per gram of RuO_2/TiO_2 sample vs. the temperature employed during the runs. From this figure, it is readily seen that, as usual for paramagnetic species,[8,9] the magnetic susceptibility per gram (χ_g') decreases as the temperature increases.

Table I shows the values for some of the runs shown in Figure 1, for the magnetic susceptibility and magnetic moment of RuO_2.

[†] Universität Zürich.
[‡] The City University.
[§] Ecole Polytechnique Fédérale.

(1) (a) Heidt, L. J.; Smith, M. E. *J. Am. Chem. Soc.* **1948**, *70*, 2476. (b) Evans, M. G.; Uri, N. *Nature (London)* **1950**, *164*, 602. (c) Buxton, G. V.; Wilford, S. P.; Williams, R. J. *J. Chem. Soc.* **1962**, 4957.

(2) (a) Kiwi, J.; Grätzel, M. *Angew.Chem., Int. Ed. Engl.* **1978**, *17*, 860; (b) *Chimia* **1979**, *33*, 285; (c) *Angew. Chem., Int. Ed. Engl.* **1979**, *18*, 624.

(3) (a) Lu, T. W. P., Srinivasan, S. *J. Appl. Electrochem.* **1979**, *9*, 269. (b) Kuhn, A. T.; Mortimer, C. J. *Ibid.* **1973**, *2*, 283. (c) Tseung, A. C.; Bevan, L. H. *Electroanal. Chem. Interface Chem.* **1973**, *45*, 429.

(4) Kiwi, J.; Kalyanasundaram, K.; Grätzel, M. *Struct. Bonding (Berlin)* **1982**, *49*, 37.

(5) (a) Kiwi, J.; Borgarello, E.; Pelizzetti, E.; Visca, M.; Grätzel, M. *Angew. Chem., Int. Ed. Engl.* **1980**, *19*, 646; (b) *J. Am. Chem. Soc.* **1981**, *103*, 6324. (c) Mills, A. *J. Chem. Soc., Dalton Trans.* **1982**, 1213. (d) Kiwi, J.; Grätzel, M.; Blondeel, G. *J. Chem. Soc., Dalton Trans.* **1983**, 2215. (e) Blondeel, G.; Harriman, A.; Porter, G.; Urwin, D.; Kiwi, J. *J. Phys. Chem.* **1983**, *87*, 2629.

(6) Hulliger, J.; Zoller, L.; Ammeter, J. *J. Magn. Res.* **1982**, *48*, 512.

(7) Bunzli, J. *Inorg. Chim. Acta Lett.* **1979**, *36*, 413.

(8) Boudreaux, E.; Muley, N. "Theory and Applications of Molecular Paragmagnetism"; Wiley-Interscience: New York, 1976.

(9) Landolt-Börstein, *Neve Serie II 8* **1976**, 26.

0002-7863/84/1506-1504$01.50/0

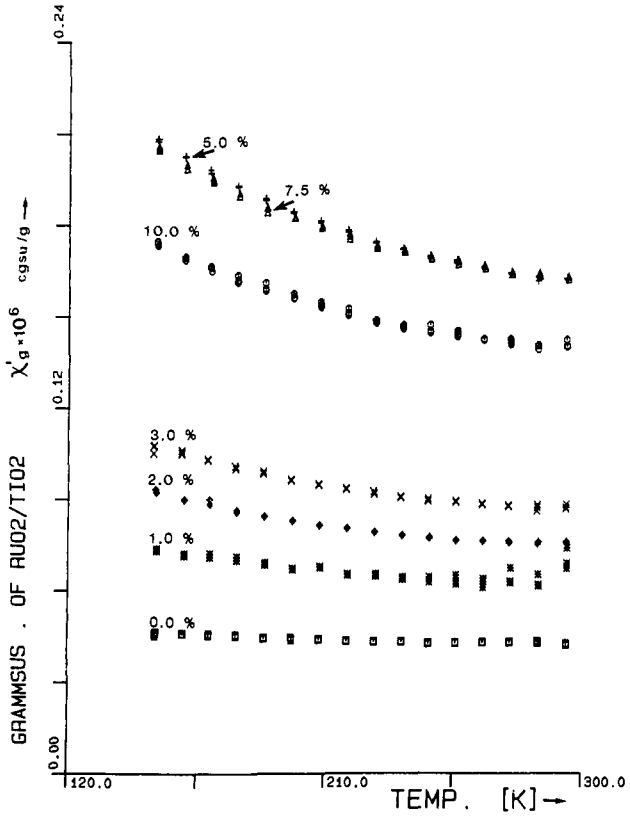

Figure 1. Variation with composition of the magnetic susceptibility per gram of RuO_2/TiO_2 samples plotted as a function of temperature.

The numerical data in this table is derived from Figure 1 by the use of relations 2, 3, and 4 shown below;[8] χ_g is the magnetic

$$\chi_g(RuO_2) = \chi_g' - (1 - S)\chi_g(TiO_2) - \chi_g^{dia}(RuO_2)S \quad (2)$$

$$\chi_m = M\chi_g \quad (3)$$

$$\mu = 2.82(\chi_m T)^{1/2} \quad (4)$$

susceptibility per gram of RuO_2, S the RuO_2 content of the sample, M the molecular weight of RuO_2, χ_m the molar magnetic susceptibility for RuO_2, μ the magnetic moment of RuO_2, and T the absolute temperature employed during these measurements.

Figure 2 shows the experimental data obtained for O_2 evolution as a function of the percent loading on TiO_2. The O_2 evolved was measured by a method reported earlier.[5] Solutions used for irradiations were 3.3×10^{-3} M Ce^{4+} in 1 N H_2SO_4. Thirty milliliters of these solutions were stirred in the presence of 12 mg of RuO_2/TiO_2 catalyst, and the observed O_2 was measured after 30 min of stirring the solution. The redox potential of the Ce^{4+}/Ce^{3+} couple in 1 N H_2SO_4 is 1.44 V (NHE) while those for H_2O/O_2 and RuO_2/RuO_4 couples are located at 1.23 and ~1.40 V (NHE), respectively. Since RuO_2 partly corrodes to RuO_4 in 1 N H_2SO_4 solution,[5] a 70% maximum is obtained (Figure 2a). The remaining Ce^{4+} is used in oxidizing RuO_2 to RuO_4.[5c,e] The increase in O_2 observed in Figure 2a when more RuO_2 particles are present allows for a greater probability of their encountering Ce^{4+} ions and reacting in a certain time interval on the catalyst surface. At this point, it is interesting to elaborate on the shape of the observed O_2 formation as a function of RuO_2 loading onto TiO_2. Figure 2b shows the variation with composition of the magnetic susceptibility measurements (χ_g') (plotted as percent loading of RuO_2 on TiO_2). The values of χ_g' have been taken from Figure 1 at 22 °C (295 K). These results show a shape for χ_g' similar to the observations reported in Figure 2a for O_2 evolution vs. percent loading of RuO_2 on TiO_2. Thus, it seems that the activity of the RuO_2/TiO_2 surface, up to the peak in catalytic activity, is a function of the RuO_2 paramagnetic sites held in exposed positions whereby they can interact with the components of the reaction to be catalyzed. The surface of the

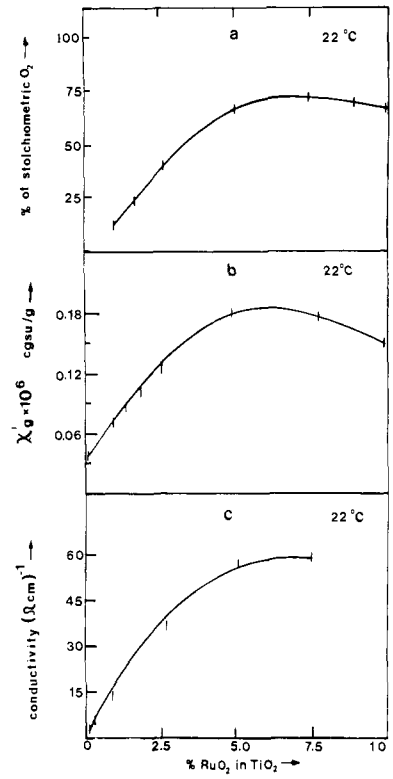

Figure 2. (a) Evolution as percentage of stoichiomeric O_2 as a function of RuO_2 loading on TiO_2. (b) Variation with composition of the magnetic susceptibility per gram of RuO_2/TiO_2 as a function of RuO_2 loading on TiO_2. (c) Variation with composition of conductivity of some RuO_2/TiO_2 powder mixtures.

TiO_2 becomes more paramagnetic at higher loadings of RuO_2. It seems that the channels for the coupling of Ce^{4+}/Ce^{3+} and H_2O/O_2 at the surface of the catalyst become enhanced, as reflected by similar changes in the correct direction for O_2 evolution and paramagnetic character of the RuO_2/TiO_2 surface. No O_2 evolution could be found when TiO_2 was not loaded with RuO_2, a further indication that paramagnetic character is necessary on the catalytic surface (as given by the RuO_2 loading) to effect efficiently the catalysis described by eq 1. The correlation between physicochemical properties reported in Figure 2a and paramagnetic properties of the system shown in Figure 2b is readily seen since the extent of O_2 evolution is proportional to the amount of RuO_2 present up to 6%. A 6% RuO_2 composition then gives a maximum for catalytic activity and paramagnetic character for RuO_2/TiO_2 samples. Loadings higher than 6% show a decrease in the observed χ_g'. This experimental observation suggests that there is an optimum ratio of RuO_2 to TiO_2 for maximum incorporation. At the point of maximum paramagnetism there are sufficient isolated sites for the oxygen precursor to be adsorbed at optimal distances for efficient O_2 evolution. Thereafter, the effectiveness of dispersion decreases, most probably due to agglomeration of RuO_2 particles on the support. Spin pairing is well-known to suppress paramagnetism and occurs when the paramagnetic centers come into proximity. Thus, this may be happening to the RuO_2 paramagnets. From Figure 2a,b it can be concluded that oxygen evolution is expected to take place on active paramagnetic surface sites and not over all the available surface area.

Figure 2c shows the variation of electrical conductivity with RuO_2 composition on TiO_2. The method of measurement and the conductivity apparatus have been previously reported.[5c,10] It is readily seen from Figure 2c that the variation of electrical conductivity with composition increases continuously with RuO_2 content up to 7.5%. The resistivity measured in Figure 2c was for RuO_2/TiO_2 powder samples pressed at 3 tons in the Teflon-brand conductivity rig. As pressure increases the grains come

(10) Tseung, A. C.; Bevan, L. H. *J. Mater. Sci.* **1976**, *5*, 604.

into closer contact, approaching the sintered state[10] and rendering a minimum value for the observed resistivity. Up to 7.5% RuO_2/TiO_2, a valid quantitative trend in conductivity vs. RuO_2 loading might be expected since each sample prepared under similar conditions possesses a similar microstructure.

This communication has reported the first quantitative study of the paramagnetism of RuO_2 islands on TiO_2. It has become clear that the paramagnetic properties of surfaces have a profound effect on chemical reactions. In reaction 1 paramagnetic species are responsible for the observed catalysis since the observed reaction goes through isolated RuO_2 islands on the surface of the catalyst. A 6% RuO_2/TiO_2 loading represents the minimum concentration (under the present experimental conditions) that provides the maximum contact for paramagnetic character as well as catalytic properties.

Registry No. RuO_2, 12036-10-1; TiO_2, 13463-67-7; water, 7732-18-5.

Mechanism of Transition-Metal-Catalyzed "Double Carbonylation" Reactions. Synthesis and Reactivity of Benzoylformyl Complexes of Palladium(II) and Platinum(II)

Jwu-Ting Chen and Ayusman Sen*

Chandlee Laboratory, Department of Chemistry
Pennsylvania State University
University Park, Pennsylvania 16802

Received October 17, 1983

In recent years, there have been a number of reports[1-4] concerning the homogeneous, catalytic formation of "double carbonylation" products through the reaction of organic halides with nucleophiles in the presence of CO (eq 1). Typical catalysts

$$RX + 2CO + Y^- \xrightarrow{\text{catalyst}} RCOCOY + X^-$$

$$R = \text{hydrocarbyl};\ X = \text{halide};\ Y^- = OH^-, NR'_2{}^- \quad (1)$$

involved were PdX_2L_2 (L = tertiary phosphines)[1,2] and $Co_2(CO)_8$.[3,4] This reaction is intriguing from a mechanistic standpoint. The first step obviously involves the formation of a metal acyl species through the oxidative addition of the organic halide to a low-valent metal species followed by the insertion of CO into the resulting metal–carbon bond. In support of this postulate, it has been shown[5] that *trans*-$PdR(X)L_2$ reacts with CO and R'_2NH to yield $RCOCONR'_2$. We also find that *trans*-$PdCOPh(Cl)(PPh_3)_2$ (**1**) reacts analogously. Thus, the intermediacy of metal alkyl and acyl species in the "double carbonylation" reaction appears to be well supported. From the metal acyl species, however, there are two mechanistically distinct pathways to the "double carbonylation" products (Scheme I), and results reported previously do not distinguish between these routes. In this paper we present direct evidence which indicates that, at least for the palladium-catalyzed system, the "double carbonylation" products are formed by a nucleophilic attack on the coordinated CO molecule[6] of a RCO–Pd–CO species to form RCO–Pd–$CONR'_2$, which then undergoes reductive elimination to give $RCOCONR'_2$ (path B).

Table I

	10^5k_1, s^{-1}	10^5k_2K, $M\ s^{-1}$
17.2 ± 0.1	8.06	0.390
25.4 ± 0.5	30.1	1.73
30.1 ± 0.1	58.1	4.32
34.2 ± 0.1	96.4	8.16

Scheme I

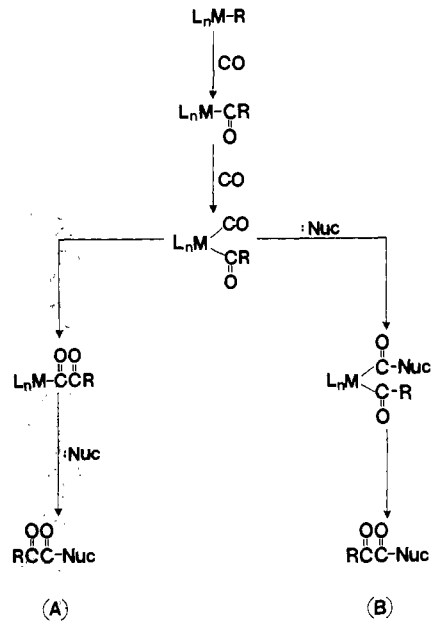

The central question concerning the mechanism of the "double carbonylation" reaction is the possible intermediacy of species such as $PdCOCOR(X)L_2$. Prior to our work the only known related compounds were *trans*-$PdCOCO_2CH_3(Cl)(PPh_3)_2$[7] and $MnCOCOR(CO)_5$ (R = CH_3, $PhCH_2$, Ph).[8] Since these compounds were not directly relevant to the reported palladium-catalyzed "double carbonylation" reactions, we were forced to synthesize one of the postulated intermediates, $PdCOCOPh(Cl)(PPh_3)_2$ (**2**) and its corresponding platinum analogue, **3**. As we shall demonstrate, the reactivity pattern of **2** was found to be significantly different from those of the manganese compounds, which have also been studied in some detail.[8]

The compounds **2**[9] and **3**[10] were prepared by the oxidative addition of PhCOCOCl to $Pd(PPh_3)_4$ and $Pt(PPh_3)_4$ respectively (eq 2). In the preparation of **2**, an excess of PPh_3 was added to the reaction mixture to retard the decomposition of the product.

$$PhCOCOCl + M(PPh_3)_4 \xrightarrow{CH_2Cl_2} \underset{\mathbf{2},\ M = Pd;\ \mathbf{3},\ M = Pt}{\textit{trans}\text{-}MCOCOPh(Cl)(PPh_3)_2} \quad (2)$$

For reactivity studies, **2** was chosen because of its relevance to the palladium-catalyzed "double carbonylation" reactions. In solution, at room temperature, **2** spontaneously decarbonylated to the corresponding benzoyl compound, **1**, and this reaction could be followed by ^{31}P NMR, IR, or vis spectroscopy. The decomposition rates were measured by monitoring the decrease in the intensity of the 494-nm band and in CH_2Cl_2 containing added PPh_3 (0.07–0.003 M) obeyed the following empirical rate equation

(1) Ozawa, F.; Soyama, H.; Yamamoto, T.; Yamamoto, A. *Tetrahedron Lett.* **1982**, *23*, 3383.
(2) Kobayashi, T.; Tanaka, M. *J. Organomet. Chem.* **1982**, *233*, C64.
(3) Francalanci, F.; Foa, M. *J. Electroanal. Chem.* **1982**, *232*, 59.
(4) Alper, H.; Des Abbayes, H. *J. Organomet. Chem.* **1977**, *134*, C11.
(5) Ozawa, F.; Yamamoto, A. *Chem. Lett.* **1982**, *865*.
(6) Nucleophilic attack on CO coordinated to transition metals is well precedented; see: Collman, J. P.; Hegedus, L. S. "Principles and Applications of Organotransition Metal Chemistry"; University Science Books: Mill Valley, CA, 1980; p 299. For specific examples involving amines as nucleophiles, see: Angelici, R. J. *Acc. Chem. Res.* **1972**, *5*, 335.
(7) Fayos, J.; Dobrzynski, E.; Angelici, R. J.; Clardy, J. *J. Organomet. Chem.* **1973**, *59*, C33.
(8) Casey, C. P.; Bunnell, C. A.; Calabrese, J. C. *J. Am. Chem. Soc.* **1976**, *98*, 1166.
(9) ^{31}P NMR (CH_2Cl_2) 16.5 ppm (s); IR (Nujol) $\bar{\nu}$ (C=O) 1680, 1650 cm^{-1}; vis (CH_2Cl_2) λ_{max} = 494 nm (ϵ = 80 $M^{-1}\ cm^{-1}$). Anal. Calcd for $C_{44}H_{35}O_2P_2ClPd$: C, 66.04; H, 4.38; P, 7.75. Found: C, 66.22; H, 4.50; P, 7.58.
(10) ^{31}P NMR (CH_2Cl_2) 20.27 ppm (1:4:1 triplet, J_{Pt-P} = 3284 Hz); IR (Nujol) $\bar{\nu}$ (C=O) 1665, 1640 cm^{-1}. Its crystal structure will be reported separately.

0002-7863/84/1506-1506$01.50/0